

EXPERIMENTAL INVESTIGATION OF HIGH PRESSURE LIQUID CO₂ RELEASE BEHAVIOUR[†]

Mark Pursell

Health and Safety Laboratory, Harpur Hill, Buxton, SK17 9JN

Initial results are presented from laboratory-scale carbon dioxide (CO₂) release experiments, which have recently been conducted at the Health and Safety Laboratory (HSL). Measurements are presented for the outflow and near-field dispersion behaviour in the expanding CO₂ jet. These are compared to model predictions in terms of the mass release rate, temperature and pressure. Both liquid and gaseous phase CO₂ releases are studied, with reservoir pressures of between 40 and 55 bar. Observations of the location of the jets shock structure are also presented. The study provides useful information for the validation of models that may be used for quantified risk assessment of Carbon Capture and Storage (CCS) infrastructure.

This publication and the work it describes were funded by the Health and Safety Executive (HSE). Its contents, including any opinions and/or conclusions expressed, are those of the authors alone and do not necessarily reflect HSE policy.

1. INTRODUCTION

Many of the CCS projects planned in the UK involve the transport of CO₂ from the capture plant to the sequestration reservoir via pipelines carrying CO₂ in its dense-phase state (i.e. as a liquid or supercritical fluid). To assess the hazards posed by releases of CO₂ from these pipelines and their associated infrastructure, it is necessary to have suitable consequence models that are experimentally validated.

Over the last 20 years, a considerable amount of research effort has been focused on understanding the behaviour of releases from pipelines containing pressurised liquids, such as liquefied petroleum gas (LPG), e.g. Richardson and Saville (1996). These releases share some features with those of CO₂, in that both involve rapid phase-change from a liquid or dense-phase state in the pipeline to (eventually) a gaseous state at atmospheric temperature and pressure. However, CO₂ is unusual in having a triple point at 5.1 bar which causes the two-phase liquid/vapour mixture to transition to solid/vapour mixture as the CO₂ expands to atmospheric pressure. Subsequently, in the high-speed CO₂ jet, the solid CO₂ particles mix with air and sublime into vapour. There is also the potential for solids to form solid agglomerations of “dry-ice”, particularly if the release is partially enclosed. These solid effects are not present in flashing releases of substances like LPG, and they present new challenges for consequence models. A schematic describing the important physical processes in a release of CO₂ from a pipeline is shown in Figure 1.

There are currently several large research projects underway which aim to produce experimental data for the validation of CO₂ consequence models. They include the European Union funded CO2PipeHaz project¹, the National Grid COOLTRANS project and the DNV-led

CO2PipeTrans project². In addition to this, the UK Health and Safety Executive (HSE) has funded the development of an experimental facility at HSL. The present paper summarises the recent findings from this new facility.

2. EXPERIMENTAL APPARATUS

The major components of the experimental facility are shown in Figure 2. They consist of a 60l jacketed pressurised feed vessel connected to a release nozzle via a flexible transfer line. The release nozzle, which is constructed from ½” compression tube components, consists of manual and actuated ball valves to allow safety shut-off and remote operation. The nozzle assembly features a compression fitting that allows different orifice sizes to be tested. Under ambient conditions the feed vessel contains a saturated two phase (gas–liquid) mixture of CO₂, where the temperature of the vessel determines the pressure and relative volume of the phases according to the PVT relationship. It is possible to obtain temperatures and pressures representative of those that may be encountered during CO₂ transportation by controlling the feed vessel temperature using the temperature-controlled jacket.

To avoid accumulation of the CO₂ in the laboratory, the releases take place inside an extraction chamber that vents to atmosphere. Temperature and pressure are recorded at two locations in the release line – at the vessel exit, and immediately before the orifice. The pressure sensors used are Kistler Type 701A that have an operating range of 0 to 250 bar and a temperature range of –150 to 240°C. An array of sixteen 1.5 mm Type K exposed-junction thermocouples were positioned downstream from the release point. The first thermocouple was located between 12.5 mm and 50 mm

¹<http://www.co2pipehaz.eu>, accessed July 2012

²<http://www.dnv.com/ccs>, accessed July 2012

[†] © Crown Copyright 2012. This article is published with the permission of the Controller of HMSO and the Queen’s Printer for Scotland.

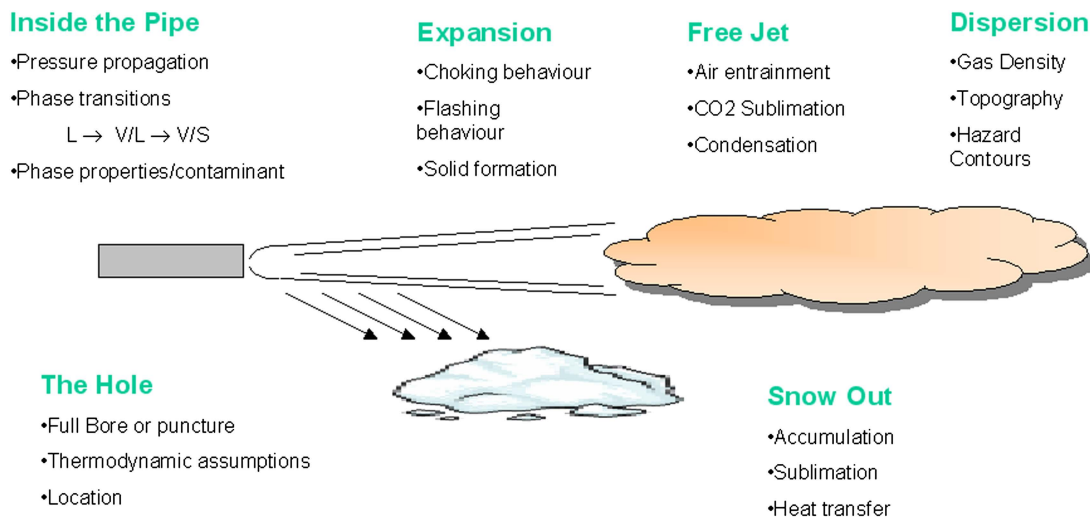


Figure 1. Overview of the physical processes involved in the release of dense-phase CO₂ from a pipeline

from the orifice (the precise location being dependent upon the orifice size), with the others are positioned at increasing intervals up to 2 m from the orifice. Data from the pressure and temperature sensors are logged using a NI cDAQ chassis that was controlled from a PC using the NI Signal Express software.

3. RESULTS

3.1. EXPERIMENTAL TESTS

The experimental facility has been used to conduct a range of tests with either saturated gaseous or saturated liquid take-off from the CO₂ feed vessel, with initial pressures ranging from 40 to 55 bar. The experimental results presented in this paper concentrate on four conditions where the release orifice was either 2 mm or 4 mm in diameter

and the supply phase was either saturated gas or liquid. The experimental conditions and measurement data are summarised in Table 1.

Figure 3 shows a typical set of measurements for pressure and mass, obtained during the release of liquid CO₂. There is very little pressure drop between the vessel and the orifice, and upon opening the actuated valve the release nozzle rapidly attains the pressure of the feed vessel. Thereafter, the feed and nozzle pressures decay rapidly before recovering to a gradually decreasing value when steady flow is established. The initial reduction in pressure occurs whilst steady flow is being established, when any non-homogenous material (CO₂ gas and air) is flushed from the flow line. Thereafter, the slow pressure decrease is due to the vaporisation within the vessel causing a cooling effect, which reduces the saturation

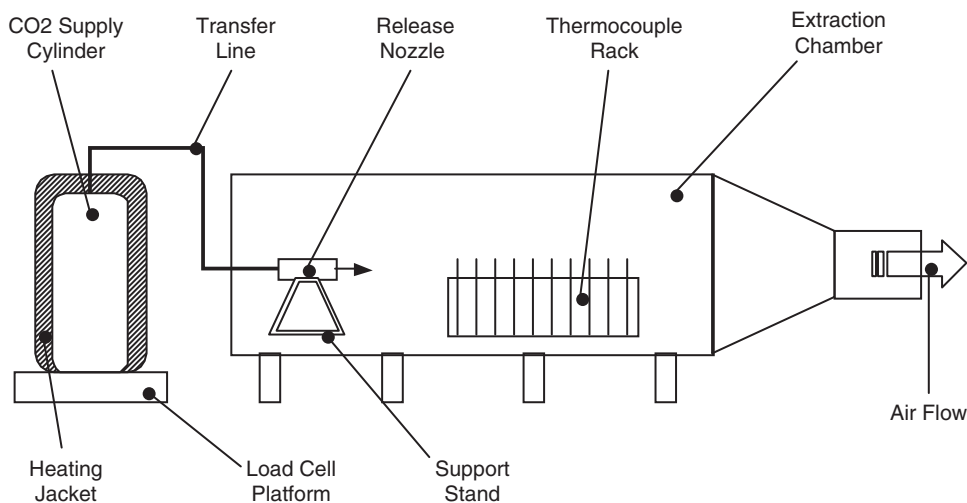


Figure 2. Schematic of the CO₂ release facility

Table 1. Measured and predicted physical properties of saturated gaseous and liquid releases of high pressure CO₂

Test ID	A	B	C	D
Feed Phase	Gas	Gas	Liquid	Liquid
Orifice size (mm)	2	4	2	4
Average Feed Pressure (bar)	44.8	40.5	54.5	49.3
Nozzle Temperature (°C)	10.4	-3.5	11.6	2.2
Orifice Temperature (°C)*	-9.6	-13.133	4.7	0.5
Nozzle Pressure (bar)	43.9	31.0	46.9	36.7
Orifice Pressure (bar)*	26.8	24.2	39.4	36.3
Orifice gas mass fraction*	0.89	0.90	0.16	0.14
Mass Flow rate – measured	0.037	0.101	0.068	0.200
Mass Flow rate – calculated*	0.040	0.143	0.083	0.315
Discharge coefficient*	0.93	0.71	0.82	0.63
Solids fraction at atmospheric plane*	0.03	0.02	0.31	0.34
Expansion zone length (mm)	10.1	17.8	10.5/16.1	19.7
Effective Diameter (mm)	12.3	21.9	18.3/18.4	28.6
Minimum Jet Temperature (°C) @ downstream distance	-48.3 @ 25 mm	-39.3 @ 37.5 mm	-82.9 @ 112.5 mm	-80.8 @ 200 mm

*Calculated quantity

pressure of the CO₂. The mass flow rate given in Table 1 has been determined from the change in vessel mass over the period of steady flow, as indicated in Figure 3. Although the pressure decreases over this period, there is only a minimal affect on the mass flow rate as the system is substantially above the critical pressure of 1.86 bar where choked flow will occur. Therefore, there is a minimal affect of the changing upstream conditions on the conditions at the exit plane. During a typical release experiment, the pressure in the vessel decreased between 3 and 5 bar.

3.2. EXPANSION BEHAVIOUR

The flow behaviour during a release can be split into three stages, as shown schematically in Figure 4. The first stage involves the flow within the pipework and vessel, from stagnation conditions up to the orifice plane. If it is at sufficiently high pressure, the flow at the orifice will choke to either the sonic velocity in the case of a gaseous release, or to a maximum flow rate condition in the case of a two-phase release. Downstream from the orifice, the fluid then expands rapidly, approximately isenthalpically, from the

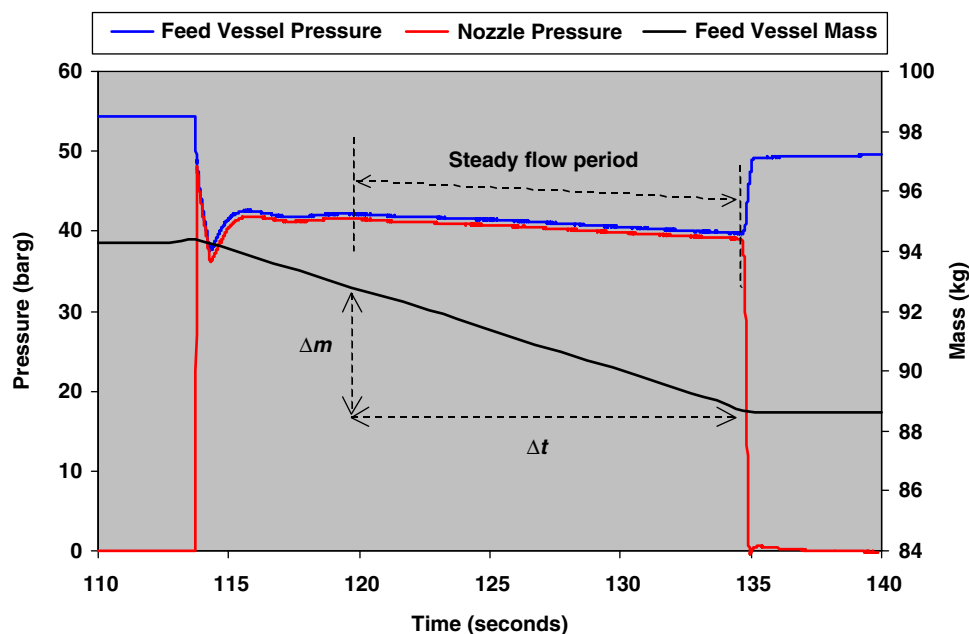


Figure 3. Experimental data trace showing the feed vessel pressure, the nozzle assembly pressure and the feed vessel mass

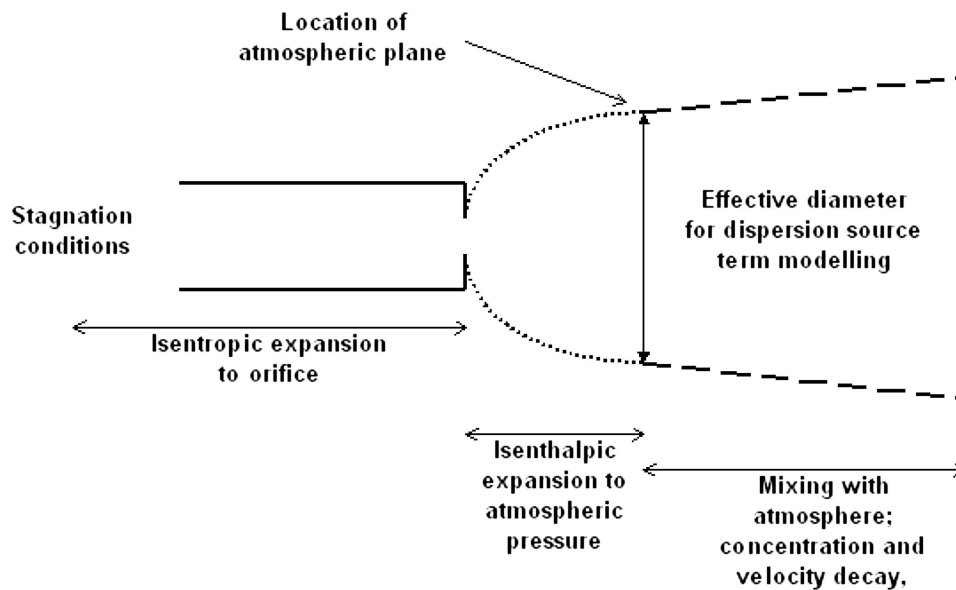


Figure 4. Schematic diagram of the expansion zone

orifice pressure to atmospheric pressure. Further still downstream, the CO₂ jet continues to expand as it entrains and mixes with the surrounding air. A more detailed description of the expansion and dispersion behaviour can be found in, for example, Witlox *et al.* (2002, 2009).

In Table 1, the measured temperatures and pressures at the orifice are compared to calculated values that have been determined assuming isentropic conditions and maximum mass flow rates at the orifice. The application of isentropic conditions to this section of the system implies an idealised flow that is adiabatic, frictionless and thermodynamically reversible. The predicted mass flow rates have had no discharge coefficient applied to them. Instead, a discharge coefficient for each test case has been calculated by comparing the experimental and predicted mass flow rates. The discharge coefficient for two-phase flow through an orifice is affected by changes in the relative quantity of gas to liquid CO₂ and variations in the flow structure. Richardson (2006) conducted an extensive investigation of two-phase flow of hydrocarbons through a variety of different orifices and reported values ranging from below 0.6 for single-phase gas releases up to nearly unity for two-phase flows with a high liquid fraction. In the present work, the quantity of gaseous CO₂ at the orifice has been calculated for each of the cases and their values are given in Table 1. For the saturated gas releases, there is condensation of 11% or 12% (mass) of the gas up to the orifice plane, and for the saturated liquid releases there is vaporisation of 14% or 16% (mass) of the liquid. The calculated discharge coefficient values presented in Table 1 are in the same range as those discussed in the work of Richardson (2006), between 0.63 and 0.93. However, the reverse trends have been produced, with higher discharge coefficients for the predominantly gaseous than the liquid-phase releases.

The mass fraction of solid CO₂ at the position downstream from the orifice where the pressure has dropped to atmospheric pressure has been calculated for each of the cases, assuming adiabatic expansion from the orifice conditions. This assumes that there is no mixing of the jet with the surrounding atmosphere so that there is minimal loss of kinetic energy. Due to the short distance and time-scales involved, and the higher than ambient pressure within this expansion zone, this is considered to be a physically valid assumption. A pressure-enthalpy chart was used to determine the solids content for each test, where the enthalpy of the system was fixed at the conditions predicted for the orifice plane and the two-phase mixture was allowed to expand to the sublimation temperature for CO₂ at atmospheric pressure of -78.5°C . For the gas releases, the final solids content was found to be very low, at 2% or 3%, whereas for the saturated liquid releases the solids content was in the range of between 31% and 34% (mass).

3.3. NEAR FIELD PROPERTIES

To validate near-field dispersion models, it is necessary to obtain good quality measurements of the flow behaviour inside the expansion region and near the point where the pressure falls to the atmospheric pressure. However, taking measurements in this region is very challenging due to the high flow velocities, rapid changes in pressure and density, and the sharp demarcations of the flow through any shock structures. Previous studies have obtained some measurements the expansion region of CO₂ jets (Khalil and Miller, 2004) by inserting probes or sensing equipment into the near-field flow. This approach is not ideal as it results in changes to the flow and may give rise to reflected shock waves. The preferred approach to is to use non-intrusive optical techniques, such as

shadowgraphy or Schlieren, where the path of the light beam passing through the expansion region is changed due to changes in the local density, temperature or pressure. However, these have their own limitations in two-phase flows, where optical access may be limited.

Figure 5 shows backlit images of the near-field jet obtained from liquid or gaseous CO₂ releases (Tests D and B, respectively, in Table 1). For comparison purposes, a sketch of the near-field structure of an under-expanded gas jet by Ewan and Moodie (1986) is also shown. For the liquid release, Figure 5a, it can clearly be seen that there is minimal light transmission throughout the entire body of the expanding jet. Additional tests conducted with a He-Ne laser that produces an intense focused point source of light showed that no light transmission through the region was possible.

The calculations discussed in the previous section predicted that a small content of the liquid CO₂ (~14% by mass) will have vaporised during the transit from the reservoir to the orifice plane. In the course of the expansion to atmospheric pressure, further vaporisation will have taken place and as the pressure passed the triple point (5.1 bar) the liquid will have become solid CO₂, reaching a final solids content of around 34% by mass when it reached atmospheric pressure. The observed attenuation of light in the expansion zone of the jet will primarily have been due to the high liquid content (down to the triple point pressure), and thereafter due to the high solids content. There is also the possibility that the liquid phase persisted beyond the triple point as a metastable phase.

In contrast to the optically opaque liquid jet, the backlit image of the gaseous release, Figure 5b, shows substantially higher levels of light transmission, with areas of attenuation which make it possible to identify the internal structure of the jet. With reference to Figure 5c, the location of the barrel shocks and the Mach disc can clearly be seen. There is an area of low light transmission in the centre of the jet, close to the orifice, which is postulated to be a two-phase

gas/liquid region above the triple point pressure. At the end of this region, the liquid content is predicted to have dropped to below 10% before freezing to solid CO₂ and thereafter sublimating, falling to a very low concentration (2%) at the atmospheric plane/Mach disc.

Despite the opacity of the liquid CO₂ jet, it is still possible to examine its shape to determine the length of the expansion zone and the effective diameter of the jet at the point where it reaches atmospheric pressure. The effective diameter may be useful for dispersion calculations, since it is often used to define the size of the pseudo-source.

For the gas releases, the expansion length has been taken as the distance from the orifice up to the visible location of the Mach disc, and the effective diameter has been determined from the jet profile at that point. In the case of the liquid releases, it is not possible to identify the location of any shock front. Therefore, the plane at atmospheric pressure has been taken to be location where the rapid expansion of jet radius changes to become a much more gradual increase. Figure 6 shows how these values have been determined. The results, presented in Table 1, show that for similar orifice sizes the lengths of the expansion zone are roughly equivalent for the liquid and gaseous CO₂ releases. However, the liquid releases result in an effective diameter that is around 30% larger than the corresponding gas release.

Future experimental work will examine the use of intrusive measurements (e.g. Pitot tubes and thermocouples), as well as non-intrusive measurements such as electrical capacitance tomography to characterise the near-field flow.

3.4. DOWNSTREAM PROPERTIES

3.4.1 Jet Temperature Profile

The temperature of the CO₂ jets was measured downstream from the release orifice at multiple locations. Figure 7 shows the axial temperature profiles in the jets for the experiments

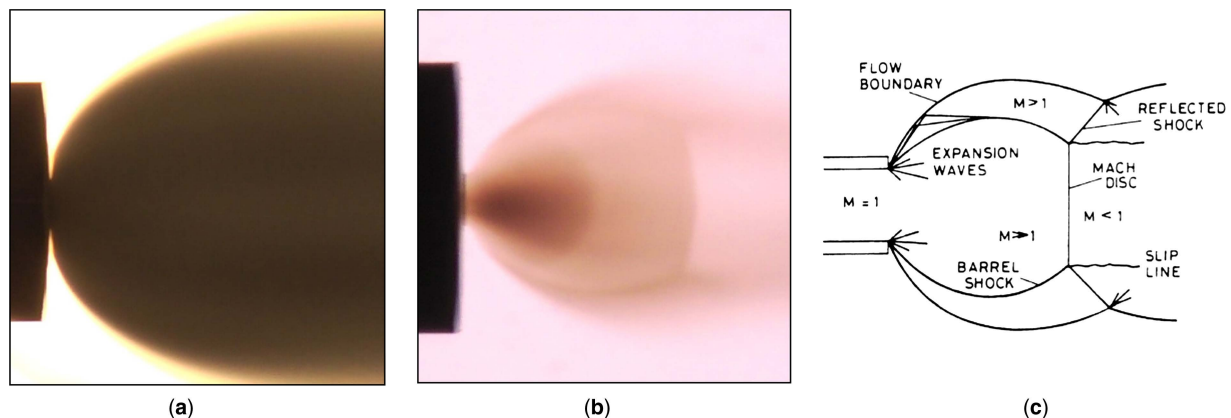


Figure 5. Images of the near-field structure of high-pressure jet releases: (a) Initially saturated liquid CO₂, 4 mm orifice, $P_0 = 49.3$ bara; (b) Initially saturated gaseous CO₂, 4 mm orifice, $P_0 = 40.5$ bara; (c) Sketch of the near field shock structure of an under-expanded gas jet (Ewan and Moodie, 1986)

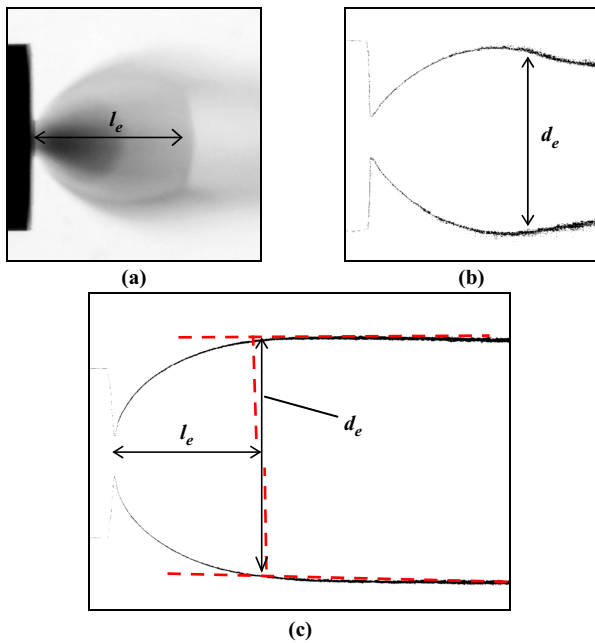


Figure 6. Shadowgraphy images from showing the location and measurement of the expansion zone length (l_e) and the effective diameter (d_e). (a) Expansion zone length measured from the orifice to the Mach disk in a gas release (b) Effective diameter at the location of the Mach disc in a gas release (c) Location and measurement of the expansion zone length and effective diameter in a liquid release

given in Table 1, where the orifice diameter was either 2 mm or 4 mm and either saturated gas or liquid CO₂ was released. In all of the cases, there was an initial reduction in the temperature followed by a steady increase with distance downstream. For the gas releases, the temperature reduction occurred over a distance of up to 25 mm from the orifice, and temperatures reached a minimum of -48.3°C for the 2 mm orifice, and -39.3°C for the 4 mm orifice. The temperature in the liquid releases reduced up to 200 mm downstream from the orifice, reaching minimum values of

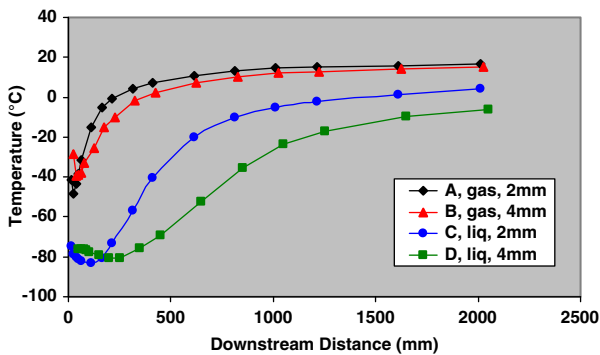


Figure 7. The downstream temperature profile for releases of saturated gas and liquid CO₂ from 2 mm and 4 mm orifices

-82.9°C for the 2 mm orifice, and -80.8°C for the 4 mm orifice.

The initial fall in temperature is a consequence of two physical effects. Firstly, in the expansion region of the jet, where the pressure is above atmospheric, the conditions are close to being in homogeneous equilibrium and the temperature therefore follows the saturation curve on the pressure-temperature phase diagram. The temperature decreases from its value at the orifice as the CO₂ expands, until it reaches a temperature -78.5°C at a pressure of 1 atm.

In the previous section, the location of the Mach disc/atmospheric plane was estimated for all four jets. Comparison of the expansion lengths to the location of measurement points in Figure 7 indicates that some of the initial measurement points may have been located inside the expansion zone, where the pressure would have been above 1 atm. In the current arrangement, the placement of thermocouples in the flow resulted in some deflection and movement of the measurement tips due to the high velocities encountered close to the orifice. Future work in this area will develop a more robust thermocouple array that will allow the temperature profiles within the expansion region to be examined in more detail.

Further downstream in the jets, the temperature in the saturated liquid releases fell below the sublimation temperature for CO₂. This cooling behaviour can be attributed to a second physical process of sublimation of the solid CO₂ particles in the entraining jet. This behaviour is examined further in the next section.

3.4.2 Sublimation Behaviour

To interpret the observed temperature profile behaviour close to the release point, an adiabatic energy balance model was developed that described the dilution of a two-phase jet of CO₂ with air. The output from this model was incorporated into a description of jet entrainment to provide predictions of the downstream temperature profile. The energy balance accounted for the condensation and freezing of water vapour (from humid air) and the sublimation of solid CO₂. Due to the small amount of water present, it was assumed that any changes in phase were instantaneous and described by the saturated vapour pressure of liquid or solid water in air at the resulting mixture temperature. The sublimation of solid CO₂ is a physically complex process that depends on the size of solid particles and the effect of local temperature and fluid flow on the mass transfer process. To simplify the present model, the mass of sublimed CO₂ (m_{CO_2Sub}) was described through a linear rate constant (k) that was related it to the quantity of diluting air (m_{air}) being mixed with the CO₂ stream, see Equation (1). In taking this approach, it was possible to give CO₂ particles a discrete lifetime in the jet.

$$m_{CO_2Sub} = km_{air} \tag{1}$$

Taking into account the above processes the energy balance was solved, together with mass continuity equations, to obtain a local temperature of the gas phase for a given quantity of diluting air. A parametric analysis

over a range of relative air dilution quantities was used to assess how the gas stream changed in temperature as more air was mixed with the CO₂ jet.

Chen and Rodi (1980) presented the following empirical formula to describe the volume concentration decay of a variable-density subsonic jet, where C is the local CO₂ concentration at a downstream distance x , C_o is the initial CO₂ concentration at the atmospheric plane (assumed here to be a value of unity), d_e the effective diameter of the source at the atmospheric plane, and x is the downstream distance from a virtual origin:

$$C(x) \approx 5 \frac{d_e C_o}{x} \left(\frac{\rho_a}{\rho_g} \right)^{1/2} \quad (2)$$

This expression was used to map the local gas jet temperatures determined through the adiabatic energy balance onto the downstream coordinate using the value of the jet dilution (concentration). To allow comparison of the model predictions with the experimental data, the effective diameter and the expansion zone length, determined in Section 3.3, were applied in Equation (2), and used to scale the experimental measurement locations relative to the virtual origin.

Figure 8 shows the application of the above model to the gaseous CO₂ releases, with three different assumed quantities of solid CO₂ initially present in the jet: 0%, 3% and 10% (by mass). The experimental data shown in Figure 8 is for Test A, which used a 2 mm orifice and was predicted to have 3% solids. The results from the energy balance model show that increasing the initial quantity of solid CO₂ in the jet leads to a delay in the onset of jet warming. Even with just 3% solids there is a noticeable effect on the temperature profile. When comparing the model results to the experimental data there is an obvious discrepancy in the initial temperature, where the model predicted initial temperatures at the sublimation temperature of CO₂ (-78.5°C), whereas the experimental measurements

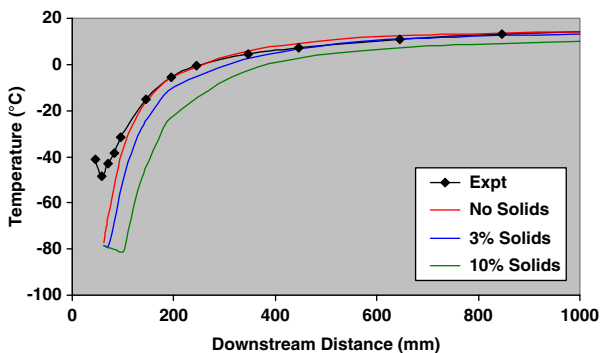


Figure 8. Comparison of the downstream temperature profiles for experimental data for saturated gas releases from a 2 mm orifice with model predictions where there was either no solid CO₂ present, or initially 3% or 10% (mass) solid CO₂ present

recorded initial temperatures in the region of -48°C. Further downstream, the experimental data and the predicted profile with no solids present coincide at around 150 mm. The model results that assumed 3% solids, as was predicted for these test conditions, converge with the experimental data after 900 mm. The third set of model results that contained 10% initial solid CO₂ content do not converge with the experimental data over the range considered.

In the analysis of the jet expansion up to the atmospheric pressure, it was assumed that the flow was adiabatic. However, if this assumption is relaxed then it is possible that the small quantities of solid CO₂ could sublime during transit through the orifice and the expansion regions due to external heat transfer, which would bring the model predictions closer to the measured values. The results suggest further investigation of the process close to orifice is required. It may be that a more robust system of temperature measurement would reveal temperatures closer to the sublimation temperature, or that an enhanced model that takes account of additional heat transfer processes would demonstrate that such low temperatures are not possible for systems where there is little or no solid CO₂ present.

In Figure 9, the effect of the rate of solids sublimation is examined for conditions that correspond to Test C, where liquid CO₂ was released through a through a 2 mm orifice. In this experiment, the temperature profile displayed an initial decrease to a temperature of -82.9°C, before increasing steadily with downstream distance. To achieve a reduction below the sublimation temperature of CO₂, the latent heat required by the CO₂ during its sublimation must be greater than the rate of heat input into the system through introduction of warmer air. The sublimation rate has been characterised through the parameter k that describes the rate of sublimation relative to the input of warm humid air. By using this constant to describe CO₂ sublimation behaviour, the best match to the experimental data was obtained with a k value of 0.2. In this case, a similar degree of initial cooling of the gas stream was obtained.

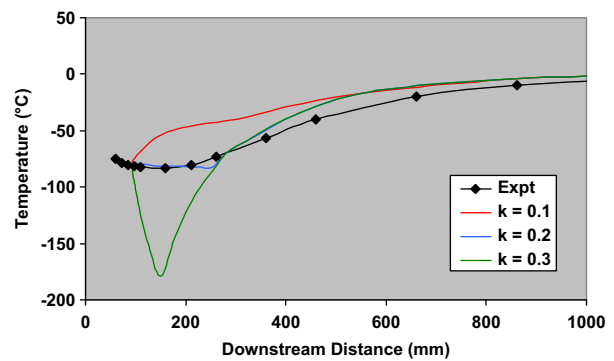


Figure 9. Examining the effect of different sublimation rates on the downstream temperature profile for liquid CO₂ releases where the initial solids contents was 34% (mass), and comparison to the corresponding experimental data for liquid release from a 2 mm orifice

However, the distance over which this occurred was slightly longer than that seen in the experiments. When the model was adjusted so that the cooling occurred over a similar distance to the experiment (with $k = 0.6$) then the minimum temperature became substantially lower at a -178°C . When k was set to a lower value of 0.1, so that sublimation occurred slowly over a longer distance, then no reduction in the temperature profile was observed. The application of a linear sublimation process is clearly too simplistic and a description of the process that changes the sublimation rate as a function of the particle size and local vapour pressure is probably needed to match the experimental data more accurately. However, the use of a sublimation rate that is directly proportional to the rate at which the jet is diluted with air does offer some insights into the overall process.

4. CONCLUSIONS

Experimental results have been presented for four laboratory-scale releases of saturated gas and liquid phase CO_2 , using orifice diameters of 2 mm and 4 mm. The data collected from these experiments has provided some useful insights into the near-field behaviour of CO_2 jets. It has been shown that the assumption of isentropic choked flow followed by isenthalpic expansion gives conditions that correlate well with experimental measurements of mass flow rate, temperature and pressure in the release nozzle and, in the case of liquid releases, with measurements in the downstream jet. The model predictions have shown relatively poor agreement with the measured temperatures when low quantities of solids are present, i.e. in the saturated gas releases. It is at present unclear whether this is a consequence of model inaccuracies or measurement errors.

Examination of the near-field flow in the expanding two-phase CO_2 jets using shadowgraphy has shown that gaseous CO_2 releases with low liquid or solid CO_2 content display a visible structure similar to under-expanded gas

jets. However, for liquid CO_2 releases, the shock structure in the near field is obscured by high concentrations of liquid and solid CO_2 , and the presence of water droplets that condense in the cold CO_2 jet from the humid ambient air. As such, further analysis of this region using optical techniques is unlikely to be successful, although tests with dry ambient atmospheres could be useful.

Future experiments using the laboratory jet release rig at HSL will concentrate on the near-field flow to measure the temperature and pressure profiles in more detail. Tests will be performed using the vessel heating jacket to obtain initial CO_2 release temperatures of between 30°C and 40°C , which are within the range of temperatures anticipated for onshore pipeline transport of CO_2 . In addition, measurements of temperature and concentration in the downstream expanding jet region will be used to assist with the validation of consequence models.

REFERENCES

- Chen C.J. and Rodi W., 1980, Vertical Turbulent Buoyant Jets – A review of Experimental Data, HMT - Science and Applications of Heat and Mass Transfer – Vol 4.
- Ewan B.C.R. and Moodie K., 1986, Structure and velocity measurements in under-expanded jets, *Combustion Science and Technology*, 45: 275–288.
- Khalil, I. and Miller, D., 2004, The structure of supercritical fluid free-jet expansions. *AIChE J.*, 50: 2697–2704.
- Richardson S.M., Saville G., Fisher S.A., Meredith, A.J., Dix, M.J., 2006, Experimental determination of two-phase flow rates of hydrocarbons through restrictions, *Process Safety and Environmental Protection* 84: 40–53.
- Witlox, H.M. and Bowen, P.J., 2002, Flashing Liquid Jets and Two-Phase Dispersion: a Review, HSE Contract Research Report 403/2001.
- Witlox, H.W.M., Harper, M., and Oke, A., 2009, Modelling of discharge and atmospheric dispersion for carbon dioxide releases, *J. Loss Prev. Process Ind.* 22: 795–802.